JACS
JOURNAL OF THE AMERICAN CHEMICAL SOCIETY

Communication

pubs.acs.org/JACS

Molecularly Resolved Images of Peptide-Functionalized Gold Surfaces by Scanning Tunneling Microscopy

Annette F. Raigoza and Lauren J. Webb*

Department of Chemistry and Biochemistry, Center for Nano- and Molecular Science and Technology, and Institute for Cell and Molecular Biology, The University of Texas at Austin, 1 University Station A5300, Austin, Texas 78712, United States

ABSTRACT: Peptide-terminated monolayers were formed through a Huisgen cycloaddition reaction between an α-helical peptide containing two propargylglycine unnatural functional groups 20 Å apart and an alkanethiol self-assembled monolayer (SAM) on a gold surface containing 25% surface density of reactive azide terminal groups. The azide- and peptide-terminated surfaces were imaged by scanning tunneling microscopy (STM) using a low tunneling current of 10 pA. On the peptide-terminated surface, oblong features ~30 Å long and ~20 Å wide were observed and attributed to individual surface-bound α-helical peptides oriented parallel to the gold surface. These features covered an area of the surface corresponding to a density of 0.11 ± 0.01 peptides nm^{-2}, compared with a theoretical density of ~0.14 peptides nm^{-2} for a fully reacted surface. Finally, no evidence of peptide aggregation was observed on either short (<10 nm) or long (~100 nm) length scales.

Integrating the function of biological molecules such as proteins with unnatural or abiological materials is now a major focus of interest in areas as diverse as sensing, chemical catalysis, nanotechnology, biofuels, and medicine.[1−10] The full integration of protein functionality with abiological materials and architectures has proved challenging because proteins often lose their three-dimensional structure or function when placed in close proximity to the unnatural chemical, structural, and electrostatic environment that occurs near inorganic surfaces and interfaces.[11−14] We recently demonstrated a novel strategy for producing biocompatible peptide-terminated surfaces in which a structured α-helical peptide is chemically bonded to an alkanethiol self-assembled monolayer (SAM) through two triazoles formed during the Huisgen cycloaddition of two azide (N_3) groups attached to the SAM and two propargylglycine residues placed strategically along the secondary structure of the peptide chain[15,16] (Figure 1).

Previous work in our lab extensively characterized these functionalized surfaces using a number of spectroscopy-based techniques.[15,16] X-ray photoelectron spectroscopy (XPS) and ellipsometry verified the formation of monolayers with a tunable bromine (and subsequent azide) density at the surface. Vibrational spectroscopy was used to confirm azide functionalization, to monitor the progress of the peptide tethering reaction, and to determine that the surface-bound peptide is oriented parallel to the gold substrate. Circular dichroism spectroscopy was used to compare the conformations of the peptide in solution and when attached to the surface; bound peptides showed a higher degree of helical character than those in solution. Finally, extensive control experiments demonstrated that peptides retained at the surface are chemically bound, not simply physisorbed to the substrate.

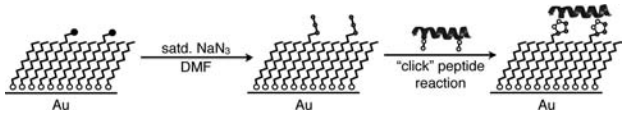

Figure 1. Schematic drawing of the surface functionalization strategy. A mixed bromine- and methyl-terminated SAM is formed on a clean gold surface and then exposed to sodium azide, resulting in a surface that contains azides and methyl terminal groups. Finally, a Huisgen cycloaddition ("click") reaction is used to tether a well-defined α-helical peptide to the azide-functionalized surface through two glycine residues modified with propargyl groups.

Until now, the interpretation of spectroscopic data acquired on the functionalized surfaces assumed that the model peptide-terminated surface shown in Figure 1 is homogeneously distributed across the surface as drawn, but surface-averaged spectroscopic measurements would not be able to distinguish homogeneously versus heterogeneously distributed functional groups or peptides. Any possible surface aggregation or heterogeneity could be a significant issue for the successful implementation of these surfaces for the controlled and reproducible adsorption of proteins; full coverage is essential, and substantial aggregation could limit further interactions between these surfaces and biomolecules of interest. To address this question, it was necessary to examine these surfaces at the molecular level.

Scanning tunneling microscopy (STM) has previously been used to characterize biomolecules, including proteins, on bare or alkanethiol-modified gold surfaces. While STM has been spectacularly successful obtaining molecular- and atomic-level resolution of crystalline and conducting surfaces, the technique is difficult to apply to biological macromolecules, which are insulating, bulky, and dynamic, and often interact with the scanning probe tip.[17,18] However, STM images have been successfully collected from biomolecules tethered directly to a conductive substrate[19,20] or inserted into a preformed, surface-bound matrix such as an ordered alkanethiol monolayer.[21,22] High-resolution images have also been obtained by codepositing peptides with additional molecules that limit aggregation or help generate a more ordered surface, though these surface architectures are more rigid and often unnatural.[23−27]

Received: September 28, 2012
Published: November 12, 2012

   dx.doi.org/10.1021/ja309632m | J. Am. Chem. Soc. 2012, 134, 19354−19357

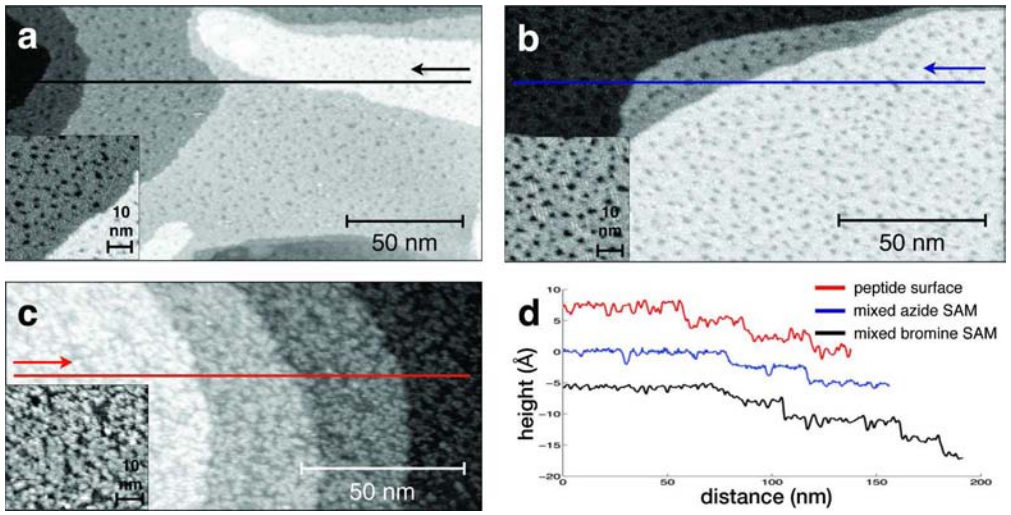

Figure 2. (a–c) STM images of functionalized surfaces after successive reaction steps: (a) mixed bromine; (b) mixed azide; (c) peptide. The insets show higher-resolution images. The images in (a) and (b) show uniform, pitted surfaces typically formed through alkanethiol self-assembly. The image in (c) displays features that cover the majority of the surface and are ~30 Å × ~20 Å in size. (d) Cross sections of the surfaces recorded along the scan lines in the directions shown in (a–c).

In this work, we used STM under conditions of ambient pressure, temperature, and humidity to characterize the functionalized SAM surface at each reaction step shown in Figure 1, resolving molecular-scale features consistent with our reaction scheme. On the final peptide-terminated surface, peptide aggregation was not evident on any length scale. Oblong features with dimensions of ~30 Å × ~20 Å were observed, which we attribute to molecular-level resolution of individual surface-bound α-helical peptides oriented parallel to the gold substrate. These images allowed us to estimate that the surface density of the peptide after chemical functionalization approached the maximum surface density possible on the basis of the size and shape of the surface-bound α-helical peptides. This is the first demonstration of molecular-level resolution of biological molecules on substrates without the imposition of additional structural order on the system through, for example, DNA base pairing or β-peptide aggregation.

A three-step procedure described in detail by Gallardo and Webb[15,16] was followed to form the peptide-modified substrates: initial formation of the chemically bound organic layer, functionalization with reactive terminal groups, and finally, peptide attachment through specific groups on the surface. A hydrogen-flame-annealed gold-on-mica substrate (Agilent Technologies) was immersed in an ethanol solution containing 0.25 mM 11-bromo-1-undecanethiol (BrUDT) and 0.75 mM 1-decanethiol (DT) for 24 h at room temperature. (All chemicals were obtained from Sigma-Aldrich and used as received, unless otherwise noted.) The 25% BrUDT/75% DT mixed surface was rinsed with ethanol, dried with a stream of N_2, and then exposed to a saturated NaN_3 solution in dimethylformamide (DMF) for 48 h at room temperature to generate a surface that was 25% N_3-terminated and 75% CH_3-terminated. The mixed azide surface was rinsed with copious amounts of water and ethanol and then dried under a stream of N_2. Finally, this surface was reacted with a model α-helical peptide (LKKLXKKLLKKLLKKXLKKL, where X is propargylglycine; PepTech Corp) in a 2:1 *t*-butanol/water solution that also contained copper sulfate, sodium ascorbate, and tris[(1-benzyl-1*H*-1,2,3,-triazol-4-yl)methyl]amine for 5 h at 75 °C. The peptide-terminated surface was rinsed with water and ethanol and dried under a stream of N_2. As-prepared surfaces were placed in N_2-purged containers and stored in the dark until they were characterized.

Images of the reacted surfaces were collected using a home-built scanning tunneling microscope controlled with commercial electronics (RHK Technology). All measurements were conducted at ambient temperature and pressure. Images were acquired at a constant tunneling current of 10 pA and a tunneling bias of 0.5 V using mechanically cut Pt/Ir tips. A high-pass fitting procedure was used to remove noise along the fast-scan direction during initial processing.[28] Additional processing to calculate the peptide surface density incorporated data from eight distinct data sets.

Figure 2 shows representative STM images of the functionalized surfaces after successive reaction steps with insets at higher resolution. The mixed-bromine and mixed-azide surfaces (Figure 2a,b, respectively) showed full monolayer coverage and small pits or "vacancy islands," typically formed during the alkanethiol self-assembly process.[29,30] These images show dense, close-packed monolayers, but defects in the gold substrate made resolving bromine or azide terminations difficult. Because there is only a one-carbon chain length difference between DT molecules and the bromine- or azide-terminated alkanethiols, these monolayers should be well-mixed, leading to a completely homogeneous distribution of the azide-terminated alkyl groups along the surface.[31]

We first analyzed these images for general information about surface quality and heterogeneity. These data show essentially no evidence of surface aggregation, aside from the infrequent appearance in Figure 2c of features significantly brighter than the surrounding area, likely due to peptides bound at only one end and oriented perpendicular to the surface.[15,16] Peptides physically absorbed but not chemically bound to the surface would give rise to streak noise in the image due to interactions with the STM tip; the absence of such features confirms the extensive earlier spectroscopic evidence that the peptides remaining at the surface are chemically bound, not just physisorbed. Furthermore, Figure 2d shows line scans across representative cross sections of the images corresponding to the mixed-bromine, mixed-azide, and peptide surfaces. The plots

dx.doi.org/10.1021/ja309632m | *J. Am. Chem. Soc.* 2012, 134, 19354–19357

show that the mixed-bromine and mixed-azide surfaces were quite smooth, with fluctuations much smaller than the height of the gold steps (2.35 Å). On the other hand, the plot line for the peptide surface is rougher, with fluctuations on the order of a couple of angstroms. Finally, the peptide-terminated surface displayed in Figure 2c was covered with regular elongated bright features that were ∼30 Å long and ∼20 Å wide. We generated an energy-minimized structure of our model α-helical peptide in the molecular modeling program Avogadro[32] and determined the dimensions of the peptide's secondary structure by measuring the end-to-end distance along the peptide's helical axis (29.6 Å) and the distance across the peptide from the termini of two opposing residues (19.6 Å). We therefore attribute these features to surface-bound α-helical peptides oriented with the helical axis parallel to the gold surface and homogeneously distributed over the substrate.

The oblong features in Figure 2c that we attribute to surface-bound peptides appeared to cover a significant portion of the flat gold surface. To quantify the extent of surface coverage, we constructed the model surface shown in Figure 3. In this figure,

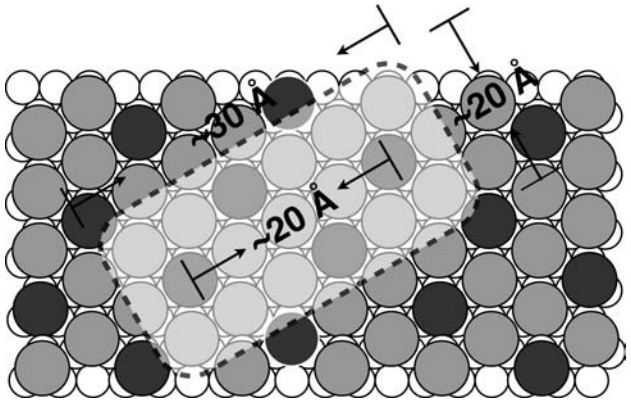

Figure 3. Cartoon of the model surface for peptide functionalization. The underlying Au(111) surface is shown in white, and the CH_3- and N_3-terminated alkanethiols in the SAM are shown in light and dark gray, respectively. The semitransparent white rectangle represents the surface area of the α-helical peptide. The approximate dimensions of the peptide are shown within the arrows. Also, the sites for peptide attachment are labeled with the distance between the reactive azides, which coincides with the distance between the alkyne termini on the propargylglycine residues of the peptide.

gold atoms from the Au(111) surface are shown in white, and the methyl- and azide-terminated alkanethiols are shown in light and dark gray, respectively. The semitransparent white rectangle on top is used to show the dimensions of the α-helical peptide. This model is based on three assumptions: (1) the concentrations of BrUDT and DT in the initial SAM-forming solution create a surface with a uniform composition; (2) the subsequently formed azide-terminated surface continues to exhibit the same ratio of reactive and nonreactive terminal groups; and (3) the two components of the SAM are homogeneously distributed across the surface. Previous XPS results confirmed that 25% Br-terminated surfaces were formed from the solutions used in these studies and that the N_3-terminated surfaces had a similar composition.[15,16] The peptide in these studies was designed in such a way that the alkyne groups on the terminal ends of the propargylglycine residues are on the same rotational plane and situated 20 Å apart, while the surface was functionalized to distribute reactive N_3 groups across the surface at similar distances to maximize peptide–surface reactions. Alkanethiol SAMs are known to form a $(\sqrt{3} \times \sqrt{3})R30°$ close-packed phase with a molecule-to-molecule spacing of 5 Å.[33,34] The initial BrUDT/DT deposition solution was prepared in such a way that the gold surface would be functionalized with one BrUDT for every three DT, placing BrUDT molecules (and consequently azide terminations) ∼20 Å apart. If each peptide is bound to the surface through two triazole linkages created via Huisgen cycloaddition, it should cover a surface area encompassing two additional azides and prevent reactions at four additional locations. According to this model structure, to functionalize the surface fully, a quarter of the azides on a 25% N_3-terminated surface would be needed, yielding a surface coverage of 0.14 peptides nm^{-2}. Using eight distinct data sets, we calculated an average density of 0.11 ± 0.01 peptides nm^{-2} based on the surface area covered by peptide features in the STM images. This demonstrates that our reaction scheme results in a density of surface-bound peptides that is near the theoretical limit established by the surface density of reactive azide groups and the known size of the α-helical peptide determined by its secondary structure.

In summary, we have shown molecular-level resolution of surface-bound structured helical peptides for the first time. Furthermore, we have demonstrated a surface functionalization scheme that produces homogeneous surfaces with no evidence of peptide aggregation and with surface coverages that are similar to theoretical values with a model surface. This scheme can be easily modified to suit any peptide with a tailored surface specifically designed for the peptide of interest. Future work will focus on further improvements in the peptide–surface interactions to maximize reaction yields and incorporation of alternately charged residues.

AUTHOR INFORMATION

Corresponding Author

lwebb@cm.utexas.edu

Notes

The authors declare no competing financial interest.

ACKNOWLEDGMENTS

This work was funded by the Army Research Office (Grant W911NF-10-1-0280). We thank Dr. Alex Kandel (Department of Chemistry and Biochemistry, University of Notre Dame) for use of the scanning tunneling microscope. L.J.W. holds a Career Award at the Scientific Interface from the Burroughs Welcome Fund and is an Alfred P. Sloan Foundation Research Fellow.

REFERENCES

(1) Barton, S. C.; Gallaway, J.; Atanassov, P. *Chem. Rev.* **2004**, *104*, 4867.
(2) Frasconi, M.; Heyman, A.; Medalsy, I.; Porath, D.; Mazzei, F.; Shoseyoy, O. *Langmuir* **2011**, *27*, 12606.
(3) Gao, Z. H.; Zhi, C. Y.; Bando, Y.; Golberg, D.; Serizawa, T. *J. Am. Chem. Soc.* **2010**, *132*, 4976.
(4) Gianese, G.; Rosato, V.; Cleri, F.; Celino, M.; Morales, P. *J. Phys. Chem. B* **2009**, *113*, 12105.
(5) Haas, A. S.; Pilloud, D. L.; Reddy, K. S.; Babcock, G. T.; Moser, C. C.; Blasie, J. K.; Dutton, P. L. *J. Phys. Chem. B* **2001**, *105*, 11351.
(6) Noll, T.; Noll, G. *Chem. Soc. Rev.* **2011**, *40*, 3564.
(7) Sarikaya, M.; Tamerler, C.; Jen, A. K. Y.; Schulten, K.; Baneyx, F. *Nat. Mater.* **2003**, *2*, 577.
(8) Seisenbaeva, G. A.; Moloney, M. P.; Tekoriute, R.; Hardy-Dessources, A.; Nedelec, J. M.; Gun'ko, Y. K.; Kessler, V. G. *Langmuir* **2010**, *26*, 9809.

(9) Wada, A.; Mie, M.; Aizawa, M.; Lahoud, P.; Cass, A. E. G.; Kobatake, E. *J. Am. Chem. Soc.* **2003**, *125*, 16228.
(10) Zrazhevskiy, P.; Sena, M.; Gao, X. H. *Chem. Soc. Rev.* **2010**, *39*, 4326.
(11) Halthur, T. J.; Arnebrant, T.; Macakova, L.; Feiler, A. *Langmuir* **2010**, *26*, 4901.
(12) Langer, R.; Tirrell, D. A. *Nature* **2004**, *428*, 487.
(13) North, S. H.; Lock, E. H.; King, T. R.; Franek, J. B.; Walton, S. G.; Taitt, C. R. *Anal. Chem.* **2010**, *82*, 406.
(14) Williams, R. A.; Blanch, H. W. *Biosens. Bioelectron.* **1994**, *9*, 159.
(15) Gallardo, I. F.; Webb, L. J. *Langmuir* **2010**, *26*, 18959.
(16) Gallardo, I. F.; Webb, L. J. *Langmuir* **2012**, *28*, 3510.
(17) Deng, Z. T.; Thontasen, N.; Malinowski, N.; Rinke, G.; Harnau, L.; Rauschenbach, S.; Kern, K. *Nano Lett.* **2012**, *12*, 2452.
(18) Madden, C.; Vaughn, M. D.; Díez-Pérez, I.; Brown, K. A.; King, P. W.; Gust, D.; Moore, A. L.; Moore, T. A. *J. Am. Chem. Soc.* **2012**, *134*, 1577.
(19) Brask, J.; Wackerbarth, H.; Jensen, K. J.; Zhang, J. D.; Chorkendorff, I.; Ulstrup, J. *J. Am. Chem. Soc.* **2003**, *125*, 94.
(20) Ceres, D. M.; Barton, J. K. *J. Am. Chem. Soc.* **2003**, *125*, 14964.
(21) Josephs, E. A.; Ye, T. *J. Am. Chem. Soc.* **2012**, *134*, 10021.
(22) Kitagawa, K.; Morita, T.; Kimura, S. *J. Phys. Chem. B* **2004**, *108*, 15090.
(23) Gong, J. R.; Yan, H. J.; Yuan, Q. H.; Xu, L. P.; Bo, Z. S.; Wan, L. J. *J. Am. Chem. Soc.* **2006**, *128*, 12384.
(24) Liu, L.; Zhang, L.; Mao, X. B.; Niu, L.; Yang, Y. L.; Wang, C. *Nano Lett.* **2009**, *9*, 4066.
(25) Mao, X. B.; Wang, C. X.; Wu, X. K.; Ma, X. J.; Liu, L.; Zhang, L.; Niu, L.; Guo, Y. Y.; Li, D. H.; Yang, Y. L.; Wang, C. *Proc. Natl. Acad. Sci. U.S.A.* **2011**, *108*, 19605.
(26) Sek, S.; Laredo, T.; Dutcher, J. R.; Lipkowski, J. *J. Am. Chem. Soc.* **2009**, *131*, 6439.
(27) Wang, Y.; Lingenfelder, M.; Classen, T.; Costantini, G.; Kern, K. *J. Am. Chem. Soc.* **2007**, *129*, 15742.
(28) Fogarty, D. P.; Deering, A. L.; Guo, S.; Wei, Z.; Kautz, N. A.; Kandel, S. A. *Rev. Sci. Instrum.* **2006**, *77*, No. 126104.
(29) Poirier, G. E. *Langmuir* **1997**, *13*, 2019.
(30) Schonenberger, C.; Sondaghuethorst, J. A. M.; Jorritsma, J.; Fokkink, L. G. J. *Langmuir* **1994**, *10*, 611.
(31) Chen, S. F.; Li, L. Y.; Boozer, C. L.; Jiang, S. Y. *Langmuir* **2000**, *16*, 9287.
(32) *Avogadro: An Open-Source Molecular Builder and Visualization Tool*, version 1.0.3; http://avogadro.openmolecules.net/.
(33) Love, J. C.; Estroff, L. A.; Kriebel, J. K.; Nuzzo, R. G.; Whitesides, G. M. *Chem. Rev.* **2005**, *105*, 1103.
(34) Schreiber, F. *Prog. Surf. Sci.* **2000**, *65*, 151.